

N 69 14924

RE-ORDER NO. 68-525

NASA CR 98714

STUDIES OF REACTION GEOMETRY IN OXIDATION AND

REDUCTION OF THE ALKALINE SILVER ELECTRODE

CASE FILE
COPY

SECOND QUARTERLY REPORT

Eliot A. Butler

Angus U. Blackham

November 15, 1968

J. P. L. 952268

Brigham Young University

Provo, Utah

STUDIES OF REACTION GEOMETRY IN OXIDATION AND
REDUCTION OF THE ALKALINE SILVER ELECTRODE

SECOND QUARTERLY REPORT

Eliot A. Butler
Angus U. Blackham

November 15, 1968

J. P. L. 952268

This work was performed for the Jet Propulsion Laboratory, California Institute of Technology, as sponsored by the National Aeronautics and Space Administration under Contract NAS7-100.

Brigham Young University
Provo, Utah

This report contains information prepared by Brigham Young University under JPL sub-contract. Its content is not necessarily endorsed by the Jet Propulsion Laboratory, California Institute of Technology, or the National Aeronautics and Space Administration.

ABSTRACT

Determination of the kinetic parameters, i_0 and α , from additional galvanostatic polarization data on the $\text{Ag}/\text{Ag}(\text{NH}_3)_2^+$ system with a newly designed cell are reported and compared with values obtained previously from the cyclic current-step (c.c.s.) method. Extension of the c.c.s. method to the initial stage of oxidation of Ag in KOH has been attempted. Specific problems encountered are discussed.

Additional data on charge acceptance as a function of applied potential confirms the general shape of the curve reported earlier and provide fine detail. Maximum values of charge acceptance are observed at 0.30 volt and 0.52 volt (Hg/HgO reference). Surface area estimations were made at 0.32 volt where the charge acceptance vs. potential curve shows a plateau. Roughness factors determined by this potentiostatic method for electropolished silver foil, foil etched with nitric acid, and sintered silver were 1.1-1.3, 3-4, and 130 respectively. These values are larger than those obtained by the constant current method. The heights of the initial current peaks on these charge acceptance curves did not correlate reasonably with roughness factors.

The influence of ultrasonic vibrations on silver electrodes is shown as an increase in charge acceptance of 5 to 25% during the $\text{Ag}/\text{Ag}_2\text{O}$ oxidation plateau as a function of current density. However, there is no observable trend in these percentages with current density, and the reproducibility of the values is from 1.0-5.1%. At a higher current density the charge acceptance for the complete oxidation (to oxygen

evolution) is increased 20-40% with vibrations. Most of the increase is observed during the second plateau, $\text{Ag}_2\text{O}/\text{AgO}$. Comparison of charge acceptance on oxidation (to oxygen evolution) with charge recovery on reduction (to hydrogen evolution) shows 96% charge recovery without vibrations and only 79% charge recovery with vibrations.

TABLE OF CONTENTS

	Page
SECTION I. Kinetic Studies of the Oxidation of Silver in Alkaline Solution	1
SECTION II. Surface Area Estimation	8
SECTION III. The Effects of Ultrasonic Vibration on the Oxidation of Silver.	14
TABLES 1-9	19
FIGURES 1-13	28
REFERENCES	41

SECTION I

KINETIC STUDIES OF THE OXIDATION OF SILVER
IN ALKALINE ELECTROLYTEIntroduction

In this section of the report the results of kinetic studies on two systems are discussed: (1) $\text{Ag-Ag(NH}_3)_2^+$. (2) $\text{Ag-Ag}_2\text{O}$. The cyclic current-step (c.c.s.) method developed by Wijnen and Smit¹ is being investigated for its possible applicability in the study of these systems because it does not have the limitations of the classical galvanostatic method² (c.g.). These limitations occur when the constant current causes a buildup of oxide on the electrode surface, thereby changing the electrode kinetics.

The first system, the $\text{Ag-Ag(NH}_3)_2^+$ electrode, was studied for two reasons. First, it provided a suitable means of checking results from the c.c.s. method against results from the c.g. method. Second, the $\text{Ag-Ag(NH}_3)_2^+$ electrode could be looked upon as an intermediate step between a system in which both the oxidized and reduced species are present as ions (for example, the ferrous ion-ferric ion system) and a system where both electroactive species are solids (silver-silver oxide). Our data in this report and in the preceding report² show that the c.c.s. method can be applied to the $\text{Ag-Ag(NH}_3)_2^+$ system.

The second system, the silver-silver oxide electrode, has yielded data which bear formal relationship to the results from measurements on a

system where the electroactive species are in solution. These data are presented in this report.

Experimental

The apparatus for the c. c. s. method is described on pages 2 and 3 of the previous report². The apparatus for the c. g. method includes a new cell (Figure 1). The cell was designed to give uniform current distribution. The need to correct for disruption of current flow lines by the Luggin capillaries was eliminated by building the capillaries into the wall of the cell. The distance extrapolation method, as described on pages 6 and 7 in the Final Report³ of JPL Contract 951911, was used to eliminate the iR drop.

Results

The $\text{Ag}-\text{Ag}(\text{NH}_3)_2^+$ System

Using the new cell (Figure 1), we have obtained galvanostatic polarization data at current densities nearly 10 times the 10 ma/cm^2 which had been the previous upper limit in our measurements. It was this lack of data at higher current densities which caused the uncertainty in the i_0 and α values obtained from the polarization data reported previously.² Plots made from data obtained with this cell are compared with other polarization data for the same system in Figure 2. The i_0 and α values determined from these plots are compared in Table 1.

The first plot on Figure 2 (points represented by \bullet) is the polarization curve made from our data by the c. g. method taken from Figure 5 of Reference 2. The values of i_0 and α determined from this plot are

1.1 ma/cm² and 0.67.

The second Tafel plot (represented by the dashed line) is based on i_o and α values of 0.66 ma/cm² and 0.5 obtained by Vielstich and Gerischer⁴ with a potentiostatic method which compared experimental current-rise versus potential plots with theoretical curves based on α and i_o . The α and i_o values which gave a theoretical curve which best fit the experimental curve were reported. However, curves based on α values of 0.5 - 0.8 would fit their experimental data equally well.

The third plot (points represented by x) was constructed from polarization data obtained by the use of the capillary which is closest to the electrode surface in the cell of Figure 1. The iR drop correction is the product of the distance between the capillary opening and the electrode surface multiplied by the potential gradient in the cell. The potential gradient is determined from measurements of the total potential drop in the cell which is 5.1 cm long. The i_o and α values determined from this plot are 4.3 ma/cm² and 0.64.

The fourth plot (points represented by o) was made from data which we obtained by use of all four capillaries of the cell of Figure 1. From this plot values of $i_o = 0.89$ and $\alpha = 0.31$ were determined. The iR drop was eliminated by the extrapolation method previously described.³ However, when high current densities are used the iR drop between any two of the fixed capillaries (0.254 cm apart) becomes large compared to the extrapolated overpotential. Thus, the error in the extrapolated overpotential becomes large compared to the overpotential. For this reason data

obtained at current densities higher than 12 ma/cm^2 were not included. This provided insufficient data to make a reliable Tafel plot. Thus the α and i_0 values obtained from this curve are not considered good. This large error in the extrapolated overpotential could, in principle, be decreased by placing the capillaries closer together and by measuring their positions more accurately. It does not appear that these efforts are necessary at this time since the data reported here and previously² are sufficient to show that the c.c.s. and c.g. methods give results which agree within experimental error on the $\text{Ag-Ag}(\text{NH}_3)_2^+$ system (see Table 1).

The data in the third and fourth plots in Figure 2 were corrected for the changes in distance between the electrode surface and the capillary which resulted from the electrochemical dissolution of the electrode. The sum of these corrections compared well with micrometer measurements of the decrease in thickness of the electrode made after a series of polarization runs.

The cell described in Figure 1 was also designed for c.c.s. measurements. To test the cell we used it for c.c.s. measurements on the $\text{Ag-Ag}(\text{NH}_3)_2^+$ system. Although some of the data were in fair agreement with the c.c.s. kinetic measurements reported previously,² others were erratic or did not give linear plots of $[\eta(\theta') - \eta(\theta'')]_0$ versus $1/\sqrt{f}$. An example of the non-linear data is shown in Figure 3. While we do not know the cause of the erratic behavior, the non-linear experimental plots in Figure 3 could be the result of reference electrode polarization. The c.c.s. method requires a counter electrode with a much larger surface area than the test electrode. If this requirement is met then the counter electrode can be considered non-

polarized and can also be used as the reference electrode. Sintered silver was used for the counter electrode to provide the large surface area in the restricted geometry of the cell. The curves in Figure 3, however, have the same shape which one would expect if the sintered silver counter electrode were replaced with silver foil. Because of this problem with the sintered electrode and the erratic results obtained with the $\text{Ag-Ag(NH}_3)_2^+$ system in the cell shown in Figure 1, the c.c.s. experiments on the $\text{Ag-Ag}_2\text{O}$ system were carried out in the wire-concentric cylinder cell described in the preceding report.²

The $\text{Ag-Ag}_2\text{O}$ System

Cyclic current-step experiments were made upon a silver electrode in KOH electrolyte at the initiation of oxidation of metallic silver. The experimental plots of $[\eta(\theta') - \eta(\theta'')]_{\theta=0.5}$ versus $1/f$ for the initial oxidation of the silver electrode in the range from about 0.05 to 11 F KOH solutions are found in Figures 4-8. A tabulation of the i_o values determined from the intercepts of these plots and the equation derived by Wijnen and Smit ($i_o = i_A RT/nF[\eta(\theta') - \eta(\theta'')]_{\theta=0.5}$) is found in Table 2.

Three observations from these data seem significant. The first is that the plots of $[\eta(\theta') - \eta(\theta'')]_{\theta=0.5}$ versus $1/f$ are linear. The second is that the i_o values obtained from the intercepts are negative instead of positive as for the ferrous-ferric¹ and the $\text{Ag-Ag(NH}_3)_2^+$ systems.² The third is that the extrapolated $[\eta(\theta') - \eta(\theta'')]_{\theta=0.5}$ measurements are approximately the same for all the KOH concentrations used. The difficulty of obtaining kinetic data from an electrode involving two solids has been noted by

Delahay.¹⁰ The c.c.s. approach appears to offer some possibility of studying the silver system just at the initiation of oxide formation.

A major difficulty encountered in the c.c.s. measurements of the silver-silver oxide electrode was with current asymmetry. If, for example, the oxidizing or positive portion of the square-wave current is greater than the negative portion, there is a net oxidizing current flow to the test electrode and a net reducing current to the counter electrode proportional to the degree of asymmetry. This results in a slow formation of Ag_2O on the silver test electrode. With the present apparatus it is possible to adjust the square wave symmetry to about $\pm 2\%$. For the experiments reported here the square wave current was adjusted so that the net current flow was reducing. This prevented the formation of Ag_2O on the test electrode but on the silver counter electrode slow formation of oxide was observed. An attempt to prevent this by passing a small direct current between a third electrode and the counter electrode resulted in very poor reproducibility in the $[\eta(\theta') - \eta(\theta'')]_{\theta=0.5}$ values for any given square wave frequency. Good reproducibility was obtained when the silver counter electrode was replaced with a platinum electrode.

It was observed that the $[\eta(\theta') - \eta(\theta'')]_{\theta=0.5}$ values drifted slowly during an equilibration period of about one hour after a new electrolyte of different KOH concentration was placed in the cell. During this time the square wave current was passed through the cell. Plots of $[\eta(\theta') - \eta(\theta'')]_{\theta=0.5}$ versus $1/\sqrt{f}$ were made several times during the equilibration period until no significant drift was observed. Once the cell had

been equilibrated the same intercept could be obtained from measurements made several hours later even though the slope of the line may have changed. The pairs of plots in Figures 7 and 8 which are labeled 1.75 ma/cm^2 resulted from measurements made at two different times. The time between the measurements for these pairs was about 12 hours.

Future Work

The kinetic investigation of the Ag-Ag₂O-AgO system will be continued. This will include measurements of the oxide layer resistance as a function of the thickness and type of oxide. Also the effect of dissolved oxygen and carbonate concentration will be studied.

SECTION II

SURFACE AREA ESTIMATION

Introduction

In earlier reports of this series,⁷ a method of surface area estimation for silver electrodes has been presented and discussed. That method is based upon the assumption that electrolytic oxidation of smooth and rough silver electrodes occurs to the same depth if the electrodes are subjected to the same actual current density (current divided by electrolytic surface area). The oxidations were conducted at constant current. Roughness factors of about 2 for silver foil electrodes etched with nitric and about 60 for sintered silver electrodes were obtained.

In our previous quarterly report,² some data for another approach were presented. The basis of this approach is the assumption that charge acceptance measured at constant potential is the same per unit of effective electrolytic surface area for smooth and rough electrodes. This assumption implies the same depth of oxidation for smooth and rough electrodes at the same potential. In this report, additional data are presented for this potentiostatic method.

Experimental

The potentiostatic unit and the electrolytic cell described in our previous quarterly report,² have been used for additional measurements. However, the potentiostat was limited by the current capacity of the booster amplifier. Additional current capacity has been provided with

the construction of a new unit which includes a booster capable of delivering 100 m.a. The circuit of this unit is shown in Figure 11.

The standard electrodes have been prepared as before by vapor deposition of silver on glass discs. The electropolished electrodes are prepared by controlled electrolysis of silver foil from a cyanide bath. The etched electrodes are obtained by placing silver foil in 6N HNO_3 for 10 seconds or 120 seconds before rinsing with distilled water. The sintered silver electrodes are available commercially from Delco Remy Company.

A suggestion was made by Malachesky and Jasinski⁵ that "the solubility of silver oxides in KOH electrolyte precludes the use of the current-time integral to estimate the amount of oxide formed as a function of the potential of formation". In our determinations the dissolution of the silver oxides has been suppressed by the use of a KOH electrolyte saturated with silver oxide.

Results and Discussion

Charge Acceptance vs. Potential

A graph of charge acceptance per unit area of smooth silver electrodes as a function of potential was included in the previous report.² Additional data have been obtained and are included in Figure 9. The general features of the curve remain the same. There is a rapid rise of charge acceptance with potential up to a value of 58 mcoul/cm^2 at 0.30 volt. This is followed by a drop in charge acceptance as the potential continues to increase. From 0.32 volt to 0.37 volt the charge acceptance appears to be constant. After a minimum at 0.42 volt the charge acceptance increases with potential

becoming quite large, 160 mcoul/cm^2 , at 0.52 volt. The charge acceptance decreases again with increasing potential. The potentials are expressed with reference to a Hg/HgO standard electrode.

Malachesky and Jasinski⁵ report similar observations on the potentiostatic oxidation of silver. They suggest that the rising parts of the curve are explained in terms of increases in the number of Ag_2O and AgO crystals respectively in the two potential ranges but that the inhibition of charge acceptance may be due to an interplay of growth and nucleation factors at the electrode surface.

Precision of Charge Acceptance Data. An estimation of the precision of the data points in Figure 9 was made by oxidation of several silver-on-glass discs at one potential, 0.32 volt. The values of charge acceptance for these electrodes are listed in Table 3. The average deviation of $\pm 15\%$ suggests some variable that we have not been able to control. In the set of determinations from which these fourteen values were taken there were four discs that were discarded because the silver film peeled away from the glass disc during the electrolytic oxidation. If some of the larger values represent discs which have imperfections but of lesser consequence than those which peeled, there may be some justification in rejecting these values. For example, with the rejection of the three largest values the average charge acceptance becomes 102 mcoul or 40 mcoul/cm^2 with an average deviation of $\pm 10\%$. If we impose a reliability of $\pm 10\%$ on the values of charge acceptance in Figure 9 the existence of maxima at 0.30 volt and 0.52 volt is still supported.

Surface Area Estimation From Charge Acceptance at Constant Potential

The potential of 0.32 volt was selected for the potentiostatic determination of charge acceptance for several kinds of silver electrodes. This potential is in a range of potentials for which the charge acceptance is constant within the error limits. The charge acceptance per unit geometrical area is larger for the electropolished and etched foil electrodes and is very much larger for the sintered silver electrode than it is for the smooth silver-on-glass electrodes. Data for these electrodes are given in Table 3.

In Table 4, surface areas calculated by the constant current method for the same electrode types are given. The surface areas for the foil and sintered electrodes are less by this method than by the constant potential method. A comparison of these values is given in Table 5 along with roughness factors. The electropolished silver foil with roughness factors 1.1 and 1.3 is slightly rougher than the vapor deposited silver-on-glass which is taken as the standard with a roughness factor of 1.00. The foil etched with nitric acid shows a marked increase in roughness factor from 2.1 with etching for 10 seconds to 4.1 with etching for 120 seconds, when measured at constant potential. The sintered silver gave roughness factors of 63 by the constant current method and 130 by the constant potential method.

Oxidative Penetration vs. Particle Size

Wales and Simon⁶ have presented photomicrographs of sintered silver electrodes at four stages of oxidation. At a magnification of 1600 X

the layer of Ag_2O is clearly shown for oxidation taken to the end of the first plateau-- $\text{Ag}/\text{Ag}_2\text{O}$. The smaller silver particles (1-5 μ) show a thicker oxide layer than do the larger particles (10-30 μ). The ratio of thicknesses appears to be approximately two.

If oxidative penetration through the surface is deeper for small silver particles than it is for flat silver foil then our surface area estimations for sintered silver electrodes may be larger than they should be.

The photographs of Wales and Simon were taken of electrodes that had been charged at the constant current estimated to require 20 hours for a complete charge. The charging rates we have used required less time. With a larger current density the difference in the thicknesses of the oxide layers may not be as great.

Attempted Surface Area Estimation

From Peak Currents

Consideration has been given to another approach for surface area estimation. With constant potential there is an initial rapid rise of current to a sharp peak. If this peak current represented an initial oxidation over the entire surface of only a monolayer, the value of the peak current would be related to the surface area. The oxidation apparently does not proceed in this way. In Table 6 data are presented which show areas calculated from peak currents. The formula was derived earlier.³

$$a (\text{Irregular}) = \frac{i_{\text{max}} (\text{Irregular})}{c.d._{\text{max}} (\text{Standard})}$$

The roughness factors of Table 6 appear reasonable for the abraded silver foil and the etched silver foil, 1.03 and 1.56 respectively. However,

a value of 1.40 for the sintered silver is unreasonable in terms of an initially complete coverage of the surface. The oxidation must start at a limited number of preferred sites.

This suggestion is supported by the curves of current flow as a function of time. In Figure 10 one observes that for each of the three silver electrodes the initial rapid increase of current is followed by a decrease. Then each of the rough electrodes shows a gradual increase in current to another maximum although much broader than the first. For the sintered silver electrode most of the charge acceptance occurs with this second current maximum.

Future Work

A model porous electrode has been described by Alkire, Grens, and Tobias.⁹ Cross sectional segments of a slightly fused coil of copper wire served as electrodes with uniform parallel pores. We plan to make similar electrodes from silver and determine their effective electrolytic surface areas by the constant potential and constant current methods. Also the initial peak current at constant potential will be measured. This information may be directly related to our observations that under some conditions a sintered silver electrode responds in about the same way as a foil electrode of the same geometric area.

SECTION III

THE EFFECTS OF ULTRASONIC VIBRATION ON
THE OXIDATION OF SILVERIntroduction

An increase in the charging capacity of a silver electrode which was subjected to ultrasonic vibrations was reported by Skalozubov and coworkers.⁸ We have observed this as an increase of rather low reproducibility in the length of the first plateau of the constant current oxidation of silver.^{2, 3}

Data have been obtained which show the per cent increase in charging capacities at different current densities and with different power densities of the ultrasonic generator.

Experiments show that the increase is more pronounced for the second plateau of the constant current oxidation than it is for the first plateau.

The decrease in time required for the reduction of an electrode at constant current from the time required for the prior oxidation of the electrode at the same current is greater if the electrode is subjected to vibrations during the oxidation and reduction than if no vibrations were used.

Experimental

Apparatus and techniques used in making charge acceptance determinations of silver electrodes at constant current are discussed in previous reports.^{2, 3}

Two ultrasonic generators were used. One, an Ultrasonics Industries Model C40 C1P-16 with an output of 80 KHz and 80 watts, had

the transducer attached to the bottom of a 1.5 liter bath. The other, a Macrosonics Corporation Model 250 FF with a tunable frequency of 700 KHz to 900 KHz and a variable power of 0-80 watts, has an immersible transducer. The transducer was fixed in position in a 12" x 12" battery jar. The jar was filled with water to a predetermined level and was thermostatted to $20.0 \pm 0.1^{\circ}\text{C}$. The experimental cell was supported in position directly above the transducer. Both the cell and the electrodes were mounted so that after having been removed from the bath they could be returned to the original position and orientation. This precaution was taken because of the highly directional character of the transducer. Figure 12 shows the placement of the cell, the electrodes, and the transducer.

Cell chambers were made from 250 ml beakers. A 3-cm diameter section in the bottom center was blown into a convex downward depression in which the Hg-HgO reference electrode was prepared. A platinum wire for electrical contact with the reference electrode was sealed through the bottom of the depression.

Another cell chamber design had the entire bottom of the beaker blown to convex downward shape. Both chamber designs are shown in Figure 13.

Silver foil electrodes which were used in measurement of the effect of the ultrasonic vibrations on the total oxidation to the evolution of oxygen were die-cut from 0.004 inch thick silver foil. The foil was cleaned with household cleanser and one side was spray painted with non-conducting

paint before the electrodes were cut. No evidence could be found that any oxidation occurred on the painted side. All other experiments used 0.010 inch thick silver foil which had been electropolished as described previously.²

Results and Conclusions

Charge Acceptance vs. Current Density

Constant current oxidations with and without vibrations at seven current densities ranging from 114 $\mu\text{amps}/\text{cm}^2$ to 456 $\mu\text{amps}/\text{cm}^2$ were compared (see Table 7). Electropolished electrodes were used and care was taken to reproduce conditions of electrode preparation and placement, solution concentration, and temperature. The small Ultrasonics Industries bath was used. Charging capacity increases of 5 to 26% were observed but no trend compared to increasing current density could be seen. (see Table 7).

Charge-Discharge

By comparing the time required to oxidize an electrode at constant current to the evolution of oxygen with the time required to reduce the electrode at that current one can show a consistent decrease in reduction time with respect to oxidation time. This difference could be caused by loss of the active mass (AgO or Ag_2O) through dissolution or disintegration. Alternatively, it could be caused by decreased current efficiency during charge. Nineteen electrodes were oxidized and then reduced under various typical conditions without vibrations. The oxidations required from seven

to twenty-five minutes but the reductions required less time than the oxidation in every case. The average decrease in reduction time compared to oxidation time was 4.3% and the average deviation was 1.3%. Eighteen runs under similar conditions except with vibrations again showed reduction times less than oxidation times in every case but the average decrease was 21.1% and the average deviation was 10.2% (see Table 8). Work is being undertaken to determine if this increased loss occurs uniformly throughout the oxidation-reduction cycle or exclusively during the oxidation or reduction of the electrode.

Increased Charge Acceptance In Second Oxidation

To determine the increase in charge acceptance during the second oxidation of silver ($\text{Ag}_2\text{O} \rightarrow \text{AgO}$) nineteen foil electrodes which had been cleaned with abrasive cleanser and painted on one side to limit oxidation to the other side were oxidized at $620 \mu\text{amps}/\text{cm}^2$. Table 9 shows the time required for the first and second oxidations and the total. The average time required for the first oxidation (T_1) was 0.78 minute with 11% average deviation. The average of the second oxidation time (T_2) was 5.87 minutes with 14% average deviation. The average of the total time ($T_1 + T_2$) was 6.65 minutes and the average deviation was 13%.

These results were compared with similar oxidations using the Macrosonics Corporation ultrasonic generator. This instrument makes use of an immersible transducer with a highly directional propagation of ultrasonic waves.

Five oxidations with each of the cell designs in Figure 13 were run. The vibrations which were directed through the bottom of the flat bottomed cell were of noticeably greater intensity than the vibrations directed through the bottom of the round bottomed cell. Apparently the round bottomed cell caused more reflection and refraction of the ultrasonic waves than did the perpendicular surfaces of the flat bottomed cell. The averages for T_1 , T_2 , and $T_1 + T_2$ for the flat bottomed cell were 0.81 minute with 14% average deviation, 8.76 minutes with 22% average deviation, and 9.57 minutes with 20% average deviation, respectively. The respective increases due to vibrations were 4%, 49%, and 44%. The round bottomed cell showed averages of 0.83 minutes for T_1 with 11% average deviation, 7.12 minutes for T_2 with 5% average deviation, and 7.95 minutes for $T_1 + T_2$ with 5% average deviation. The increases due to vibrations were 6%, 21%, and 20% respectively. These are much lower (except T_1) than the increases in the flat bottomed cell in accordance with the observed decreased power of vibrations in the round bottomed cell. These data are presented in Table 9.

Table 1

Comparison of Kinetic Data Obtained by the Galvanostatic Polarization

Method and by the Cyclic Current-step Method on the $\text{Ag}-\text{Ag}(\text{NH}_3)_2^+$

Description of run	i_A ma/cm^2	α
1. Plot #1 of Fig. 2 in this report (from reference 2 Fig. 5)	1.07	0.67
2. By Vielstich and Gerischer ⁴ (plot #2 of Fig. 2 in this report	0.66	0.50
3. Plot #3 of Fig. 2 in this report	4.3	0.64
4. Plot #4 of Fig. 2 in this report	0.89	0.31
5. C.c.s. data from reference 2	0.73	0.82

Table 2

Results of Measurements by the C. C. S. Technique
on the Ag-Ag₂O System

[KOH]	i_A (ma/cm ²)	intercept of $[\eta(\theta') - \eta(\theta'')]_{\theta=0.5}$ (mv)	i_O (ma/cm ²)
10.85 <u>F</u>	1.75	-44	-1.1
10.85 <u>F</u>	0.87	-22	-1.1
5.43 <u>F</u>	1.75	-45	-1.0
5.43 <u>F</u>	0.87	-23	-0.98
1.085 <u>F</u>	1.75	-39	-1.2
1.085 <u>F</u>	0.87	-20	-1.1
0.543 <u>F</u>	1.75	-52	-0.87
0.543 <u>F</u>	0.87	-25	-0.90
0.0543 <u>F</u>	1.75	-50	-0.90
0.0543 <u>F</u>	0.87	-30	-0.75

Table 3

Charge Acceptance at Constant Potential of Silver Electrodes of Varying Surface Roughness.

Potential: 0.320 ± 0.003 volts. Conditions: Potential, 0.320 ± 0.003 volts.

Electrode Type	Geometric Area of Electrode (cm ²)	Charge Acceptance Several Determinations (millicoulombs)		Average Value (mcoul)	Charge Acceptance per Unit Area (mcoul/cm ²)	Average Deviation (%)	Calculated Surface Area
Silver-on-Glass (vapor deposition)	2.54	117	96	101	43	± 15	2.54 (Standard)
		108	108	98			
		152	88	86			
		131	141	116			
		91	98				
Electropolished Foil	2.63	136	131	170	54	± 16	3.29
		157	155	106			
Foil Etched in 6N HNO ₃ (120 sec.)	2.63	483	496	448	177	± 5	10.7
		437					
Foil Etched in 6N HNO ₃ (10 sec.)	2.63	242	235	268	92	± 10	5.6
		218					
Sintered Silver Electrode Soaked in KOH (Delco Remy)	0.688	3700		3610	5570	± 5	88.6
		4090		3940			

Table 4

Surface Area Estimation of Silver Electrodes of Varying Surface Roughness

by the Constant Current Method.

Electrode Type	Geometric Area of Electrode (cm ²)	Applied Current (μ amps)	Plateau Length (min)	Dtms (cm ²)	Surface Area	
					Average Value (cm ²)	Average Deviation (%)
Silver-on-glass (vapor deposited)	2.54	—	—	—	2.54	—
Electropolished Foil	2.63	300	15.83	3.00	2.86	<u>+3%</u>
		300	15.21	2.76		
		300	15.68	2.81		
Foil Etched in 6N HNO ₃ (120 sec.)	2.63	1200	8.25	8.89	8.21	<u>+5%</u>
		1200	6.50	7.89		
		1200	6.75	8.06		
Foil Etched in 6N HNO ₃ (10 sec.)	2.63	500	6.55	3.31	3.44	<u>+3%</u>
		500	7.00	3.48		
		500	7.50	3.55		
Sintered Silver Electrode Soaked in KOH Delco Remy	0.688	3500	20.25	43.6	43.2	<u>+2%</u>
		3500	18.00	42.0		
		3500	21.50	44.0		

Table 5

Comparison of Constant Current and Constant Potential Methods for
Determining Surface Areas and Roughness Factors of Silver Electrodes

Electrode Type	Geometric Area of Electrode (cm ²)	Effective Electrolytic Surface Area (cm ²)		Roughness Factor	
		Constant Potential Method	Constant Current Method	Constant Potential Method	Constant Current Method
Silver-on-glass (vapor deposition)	2.54	2.54	2.54	1	1
Electropolished Foil	2.63	3.29	2.86	1.25	1.09
Foil Etched in 6N HNO ₃ (120 sec.)	2.63	10.7	8.21	4.1	3.1
Foil Etched in 6N HNO ₃ (10 sec.)	2.63	5.6	3.44	2.1	1.3
Sintered Silver Electrode (Delco Remy)	0.688	88.6	43.2	130	63

Table 6

Surface Area Estimation From Peak Currents in the Oxidation of
Silver Electrodes at Constant Potential (0.320 ± 0.003 volts vs.
Hg/HgO reference)

Electrode Type	Geometric Area of Electrode (cm ²)	Observed (ma)	Peak Current Average Value (ma)	Average Deviation %	Area Calculated from Peak Current	Roughness Factor
Silver-on-glass	2.54	4.00 4.00 3.95 4.05	4.00	± 0.5	2.54	1.00
Silver Foil Rubbed with Abrasive Paper	2.63	4.00 4.10 4.20 4.05	4.09	± 1.5	2.7	1.03
Foil Etched in 6N HNO ₃ (120 sec.)	2.63	6.75 5.80 6.40 6.05	6.25	± 5	4.1	1.56
Sintered Silver Electrodes Soaked in 0.1 N KOH (Delco Remy)	0.688	5.80 5.10 5.60 5.80	5.57	± 4	0.96	1.40

Table 7

A Comparison of Increases in Charging Capacities
at Seven Current Densities

Number of Runs	Current Density ($\mu\text{amps}/\text{cm}^2$)	Vibrations ?	Average Oxidation Time (minutes)	Per cent Average Deviation	Per cent Increase
6	114	No	14.93	3.2	5.2
5	114	Yes	15.71	1.3	
6	152	No	9.32	1.2	5.9
5	152	Yes	9.87	1.7	
6	190	No	6.36	1.8	12.1
6	190	Yes	7.13	4.9	
6	228	No	4.78	1.0	20.7
6	228	Yes	5.77	3.3	
5	304	No	3.05	1.6	13.4
5	304	Yes	3.46	4.6	
6	380	No	2.10	4.8	25.7
5	380	Yes	2.64	3.2	
5	456	No	1.55	5.1	21.9
4	456	Yes	1.89	1.5	

Table 8

Oxidation and Reduction of Silver Foil Electrodes With and Without
Vibrations under Various Typical Conditions

Without Vibrations			With Vibrations		
Oxidation Time	Reduction Time	% Decrease	Oxidation Time	Reduction Time	% Decrease
9.19	8.79	4.4	6.92	5.00	27.7
10.46	10.18	2.7	7.25	4.93	32.0
10.91	10.60	2.8	7.83	6.47	17.4
11.26	10.62	5.7	8.63	6.85	20.6
11.32	10.72	5.3	9.13	7.92	13.3
11.32	10.90	3.7	10.11	8.72	13.7
11.85	11.26	5.0	10.16	8.65	14.9
17.00	16.21	4.6	10.49	6.69	36.2
17.94	17.08	4.8	10.62	9.51	10.5
17.95	17.41	1.3	10.68	10.01	6.3
18.14	16.98	6.4	10.77	9.22	14.4
18.28	17.50	4.3	14.24	12.54	11.9
18.74	17.69	5.6	15.02	12.57	16.3
18.79	17.92	4.6	18.93	16.96	10.4
18.93	18.11	4.3	19.58	12.00	38.7
18.94	18.42	2.7	20.73	18.35	11.5
18.98	18.58	2.1	23.14	11.56	50.0
19.13	18.73	2.1	24.44	15.98	34.6
19.98	18.23	8.8			
Average 4.3			Average 21.1		
Average deviation 1.3%			Average deviation 10.2%		

Table 9

Oxidation of Silver Foil to the Evolution of Oxygen at Constant

Current with and without Ultrasonic Vibrations.

Area: 1.29 cm^2 . Temperature: $20.0^\circ \pm 0.1^\circ \text{C}$.Current Density: $620 \frac{\mu\text{amps}}{\text{cm}^2}$

Without Vibrations			With Vibrations		
			Flat-bottomed Cell		
First Plateau T_1 in min.	Second Plateau T_2 in min.	Total Oxidation $T_1 + T_2$ in min.	First Plateau T_1 in min.	Second Plateau T_2 in min.	Total Oxidation $T_1 + T_2$ in min.
0.70	5.07	5.77	0.68	9.30	9.98
0.86	5.14	6.00	0.68	5.65	6.33
0.63	4.82	5.45	1.04	7.00	8.04
0.74	5.68	6.42	0.81	11.16	11.97
0.86	4.39	5.25	0.86	10.67	11.53
0.60	5.62	6.22	average	average	average
0.87	4.86	5.73	0.81	8.76	9.57
0.73	5.64	6.37	14% a.d.	22% a.d.	20% a.d.
0.90	6.84	7.74			
0.70	6.98	7.68	4% increase	49% increase	44% increase
0.74	5.01	5.75			
0.81	6.72	7.53			
0.96	6.14	7.10	Round-bottomed Cell		
0.77	8.35	9.12	T_1	T_2	$T_1 + T_2$
0.87	5.08	5.95	0.83	6.55	7.38
0.88	6.97	7.85	0.76	6.92	7.68
0.86	6.44	7.12	1.05	7.23	8.28
0.87	6.24	7.11	0.74	7.88	8.62
0.74	5.46	6.20	0.77	7.03	7.80
average	average	average	average	average	average
0.78	5.87	6.65	0.83	7.12	7.95
11% a.d.	14% a.d.	13% a.d.	11% a.d.	5% a.d.	5% a.d.
			6% increase	21% increase	20% increase

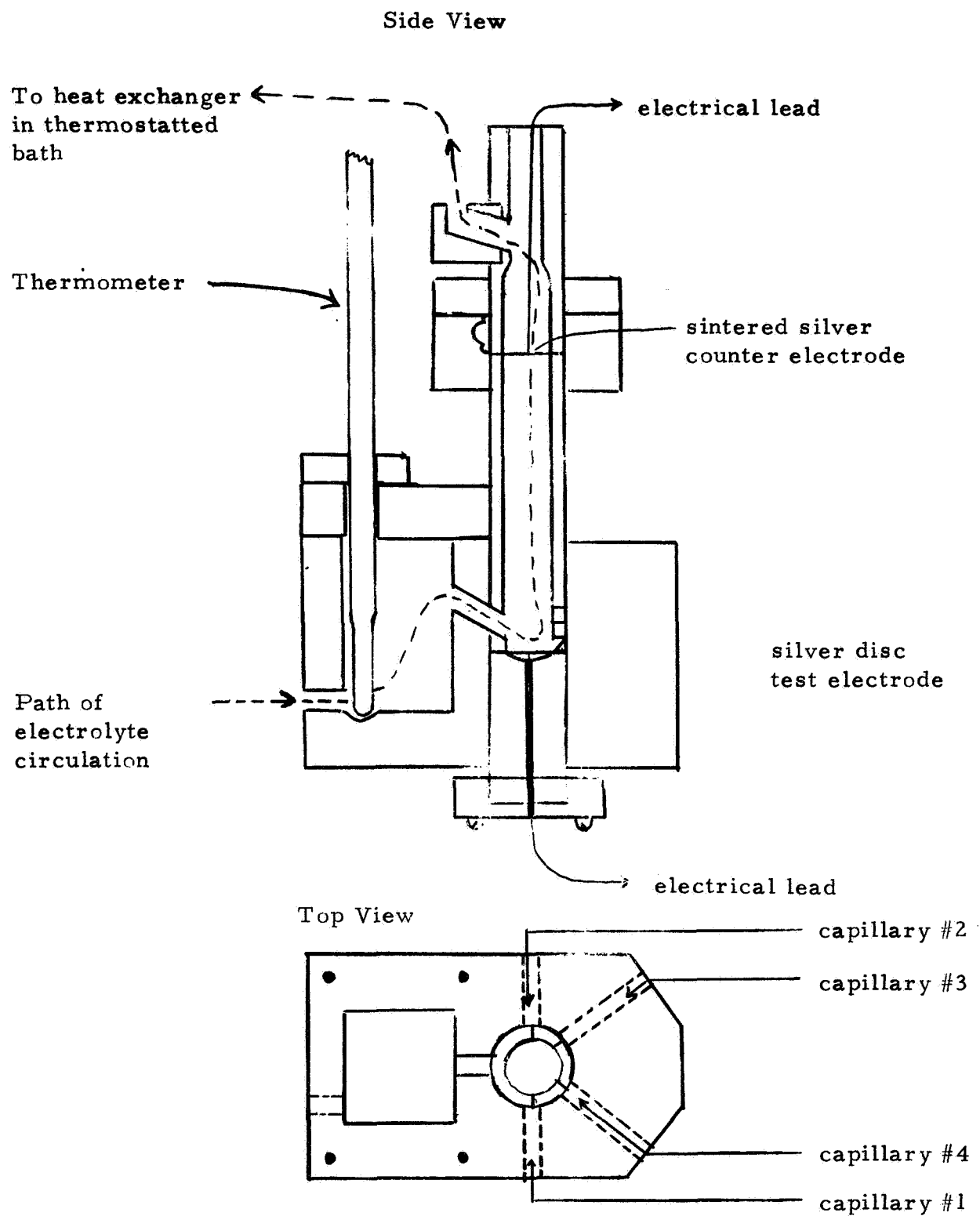


Fig. 1. --Schematic of test cell designed for c.g. and c.c.s. kinetic studies

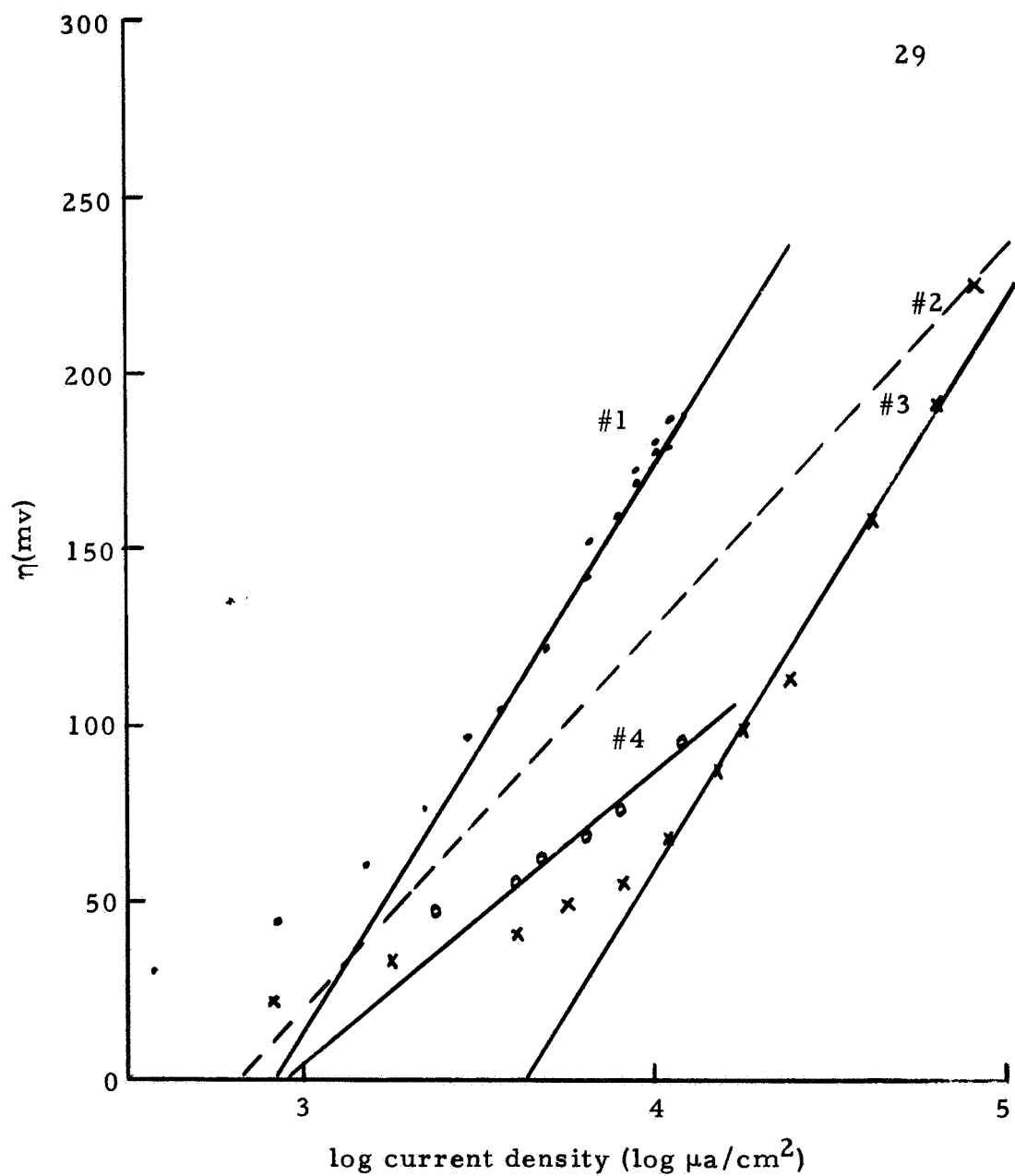


Fig. 2. --Comparison of Classical galvanostatic polarization data obtained by different methods on the $\text{Ag-Ag}(\text{NH}_3)_2^+$ system.

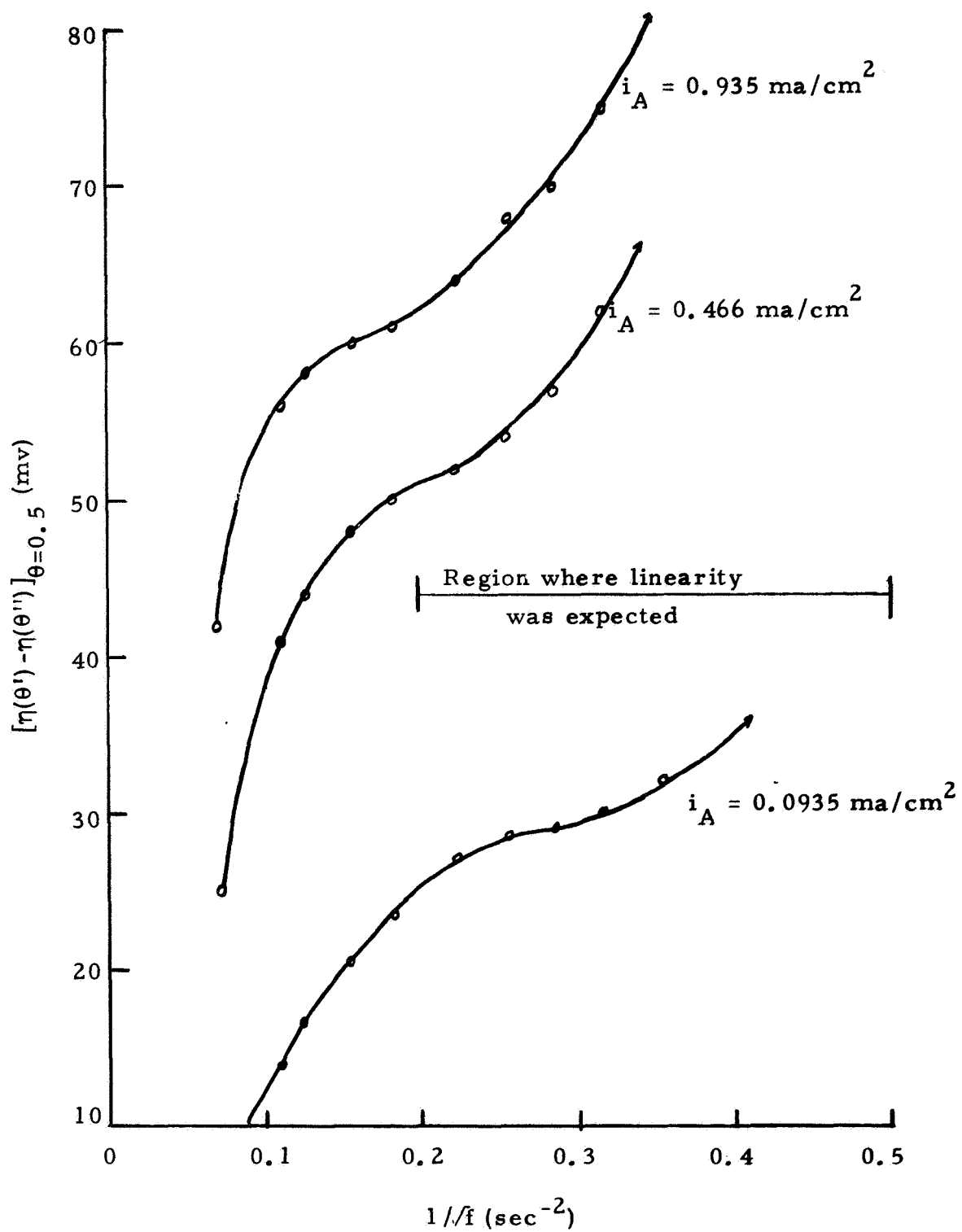


Fig. 3. --Nonlinear c.c.s. data obtained with the cell described in Fig. 1.

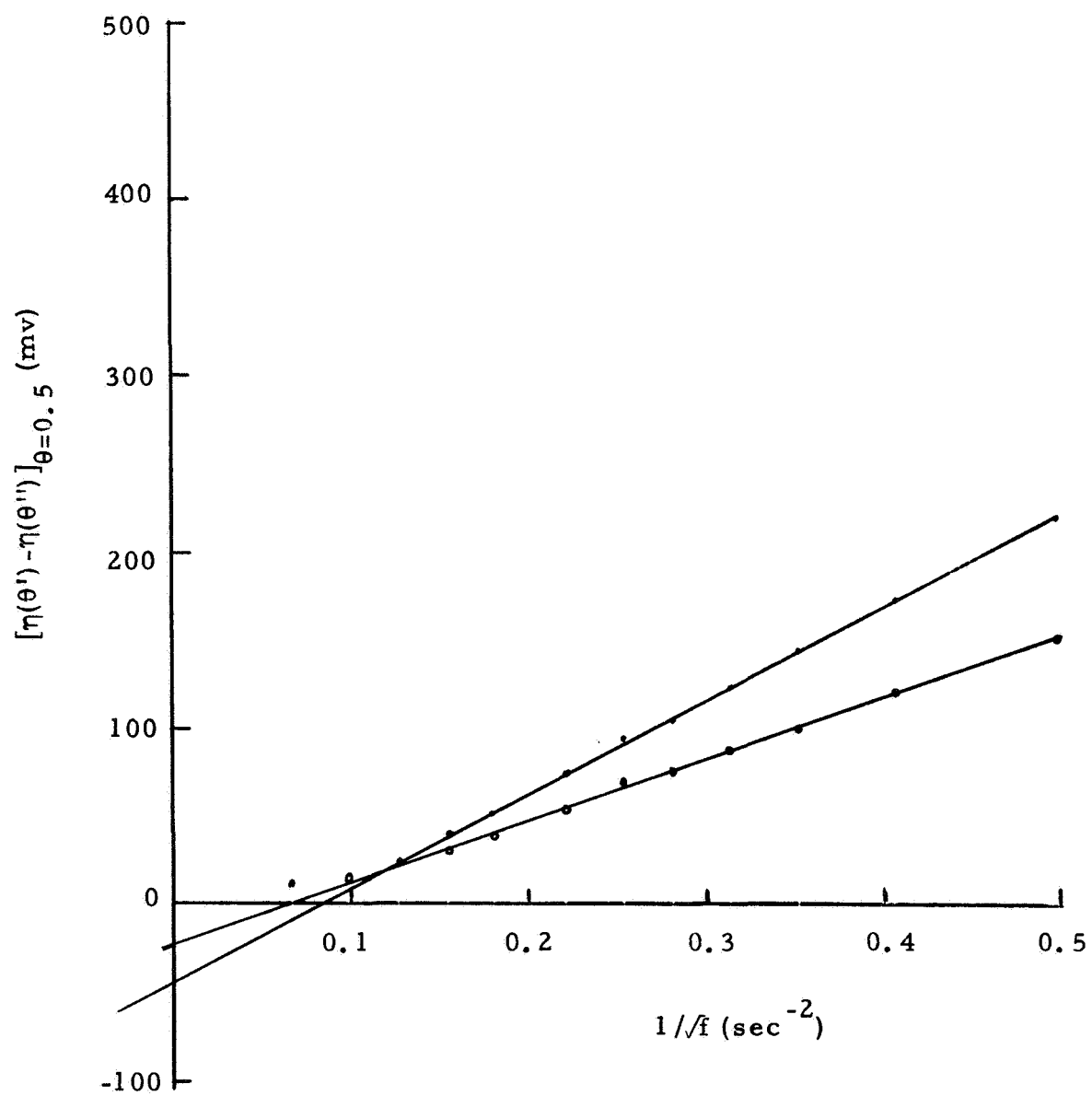


Fig. 4. --C. c. s. data of the Ag-Ag₂O system in 10.85 F KOH

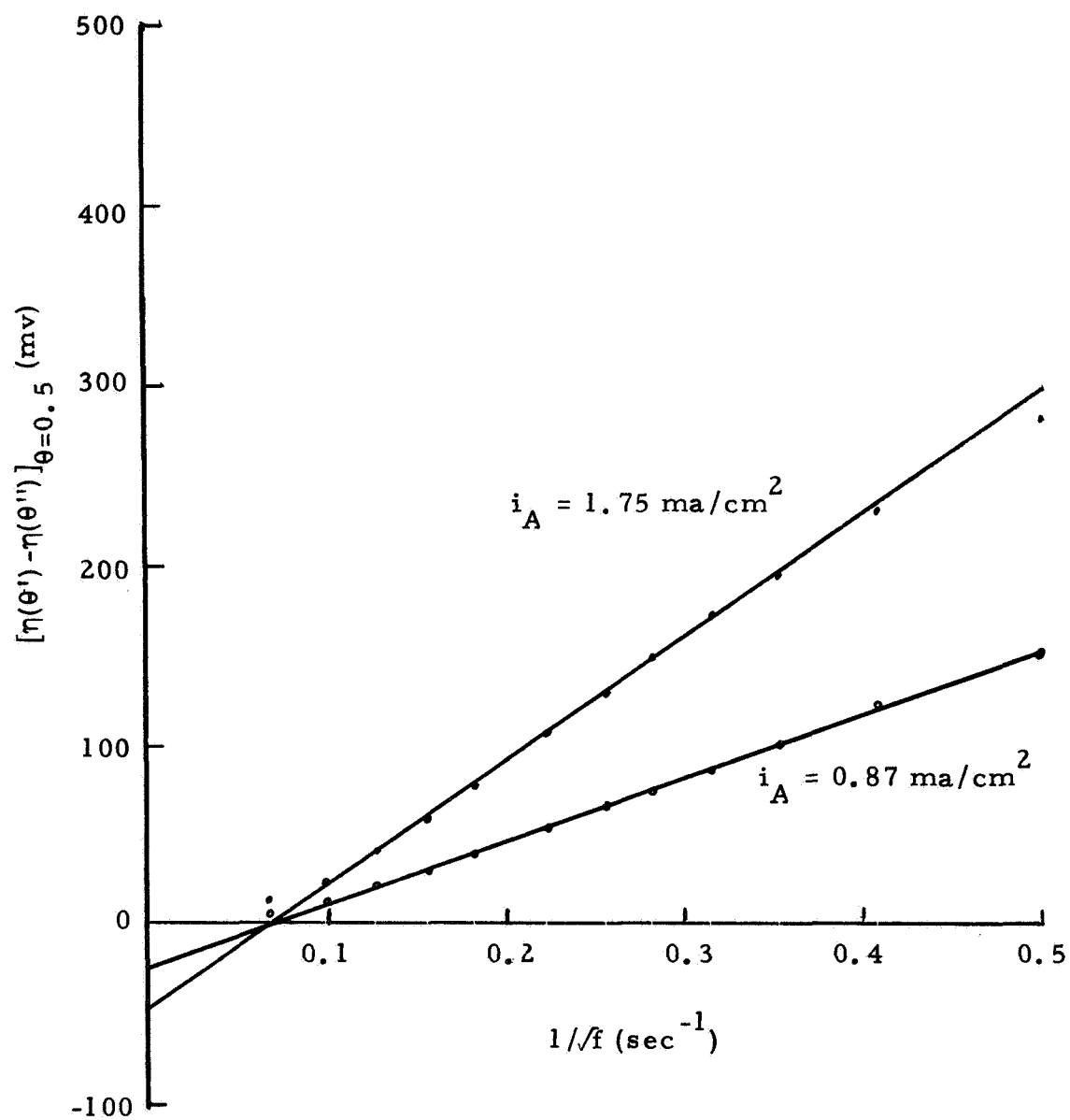


Fig. 5. --C.c.s. data of the Ag-Ag₂O system in 5.43 F KOH

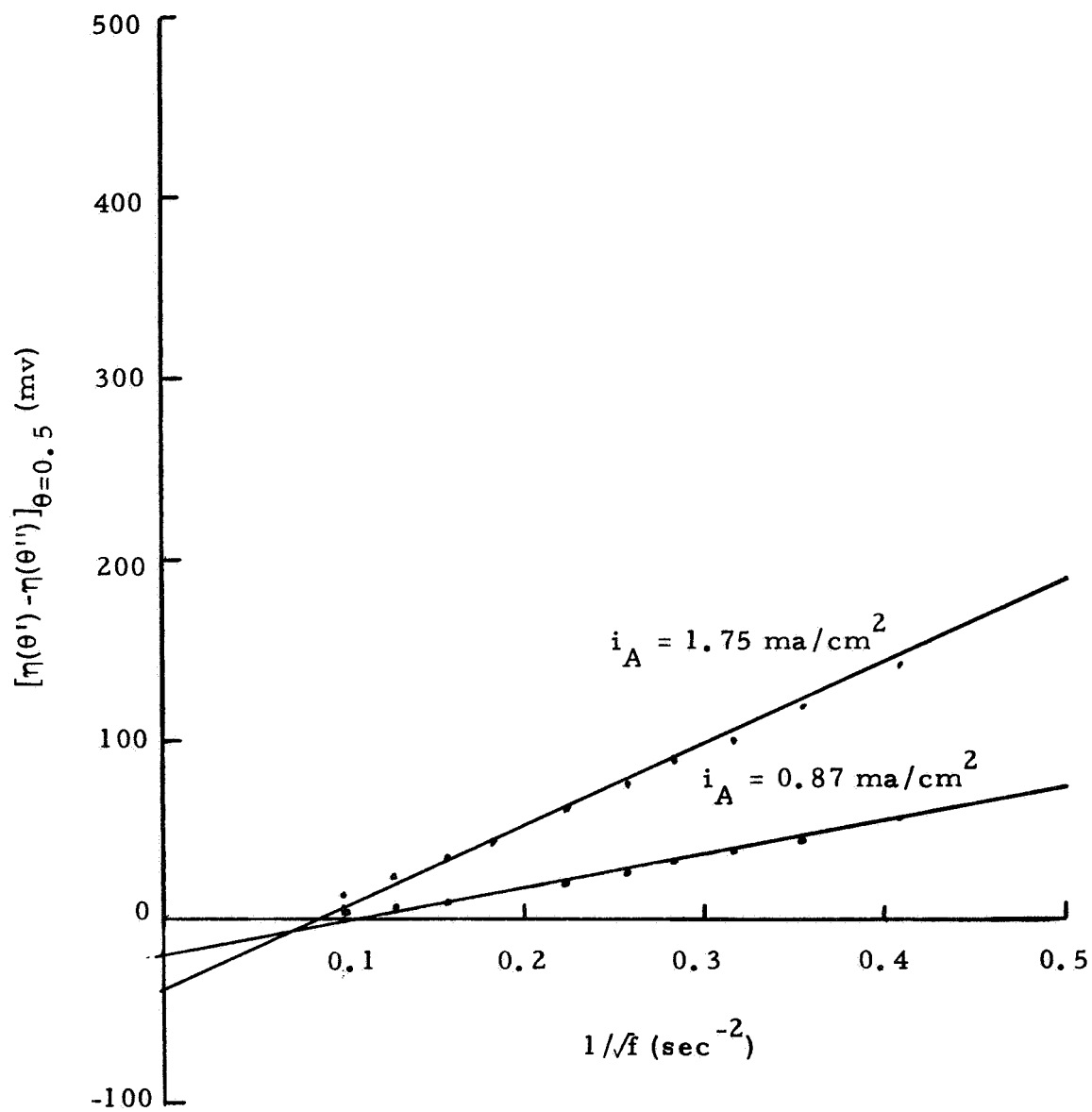


Fig. 6. --C. c. s. data of the Ag-Ag₂O system in 1.085 F KOH

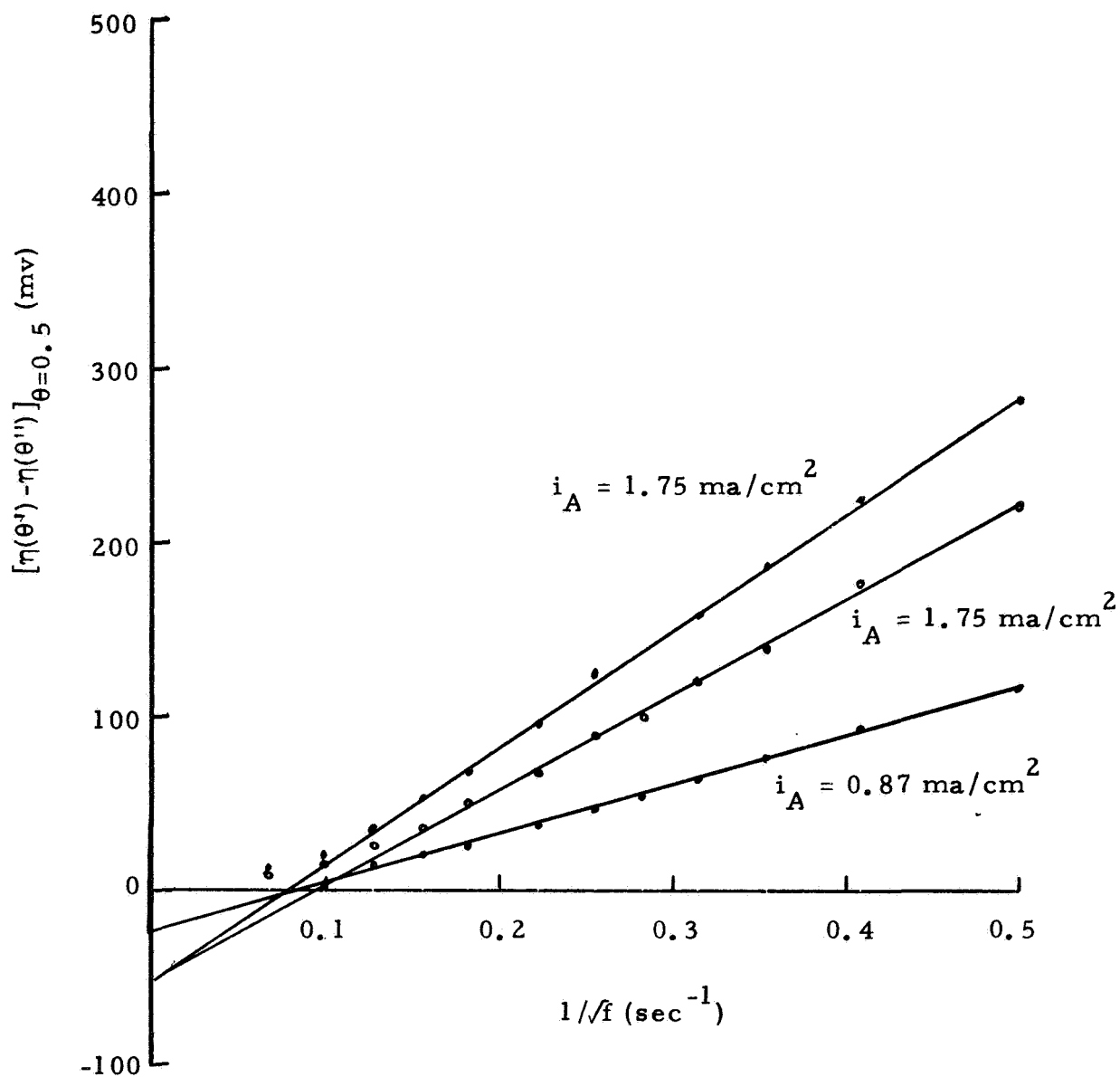


Fig. 7. --C.c.s. data of the Ag-Ag₂O system in 0.543 \underline{F} KOH

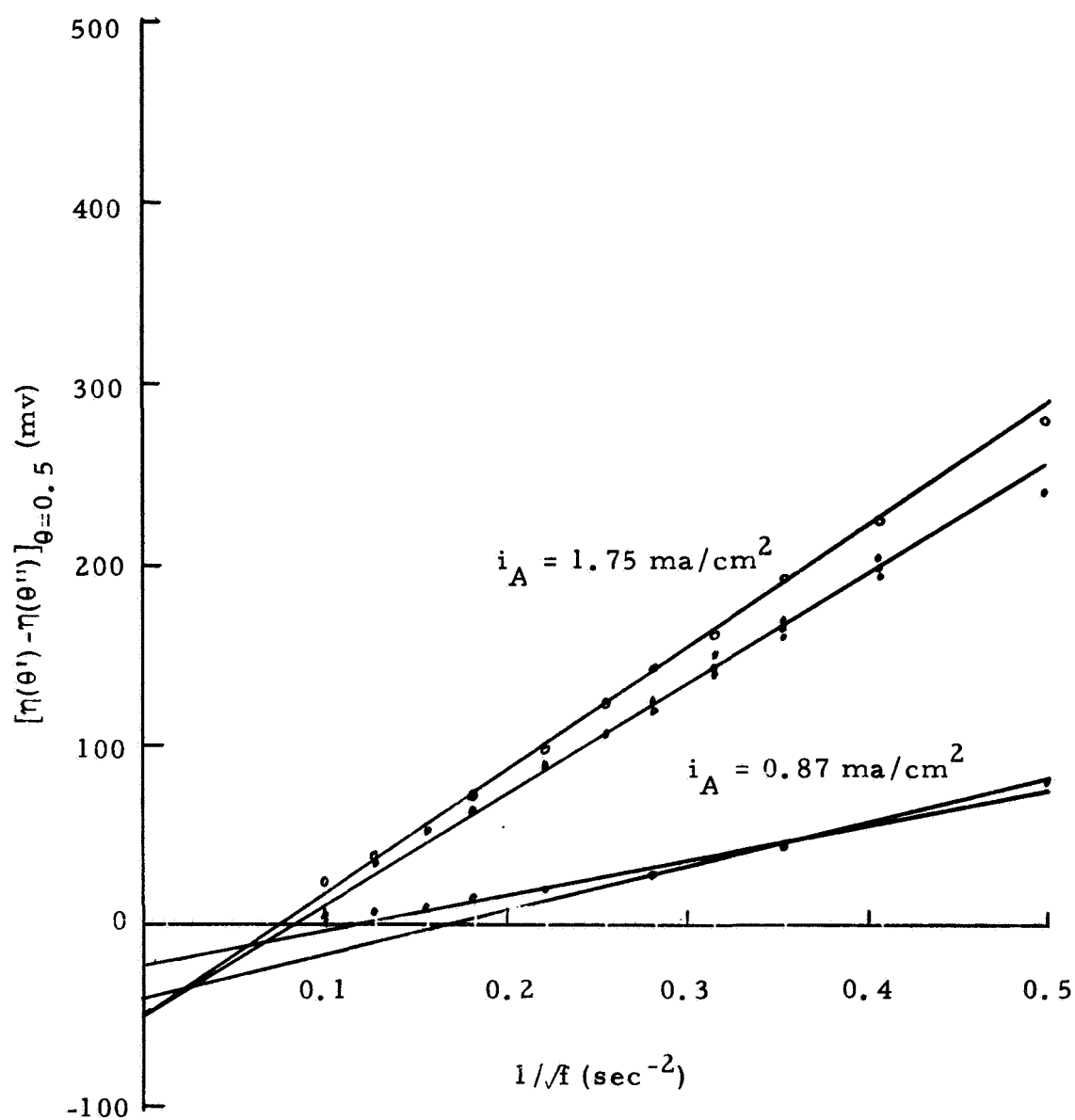


Fig. 8. --C.c.s. data of the Ag-Ag₂O system in 0.0543 F KOH

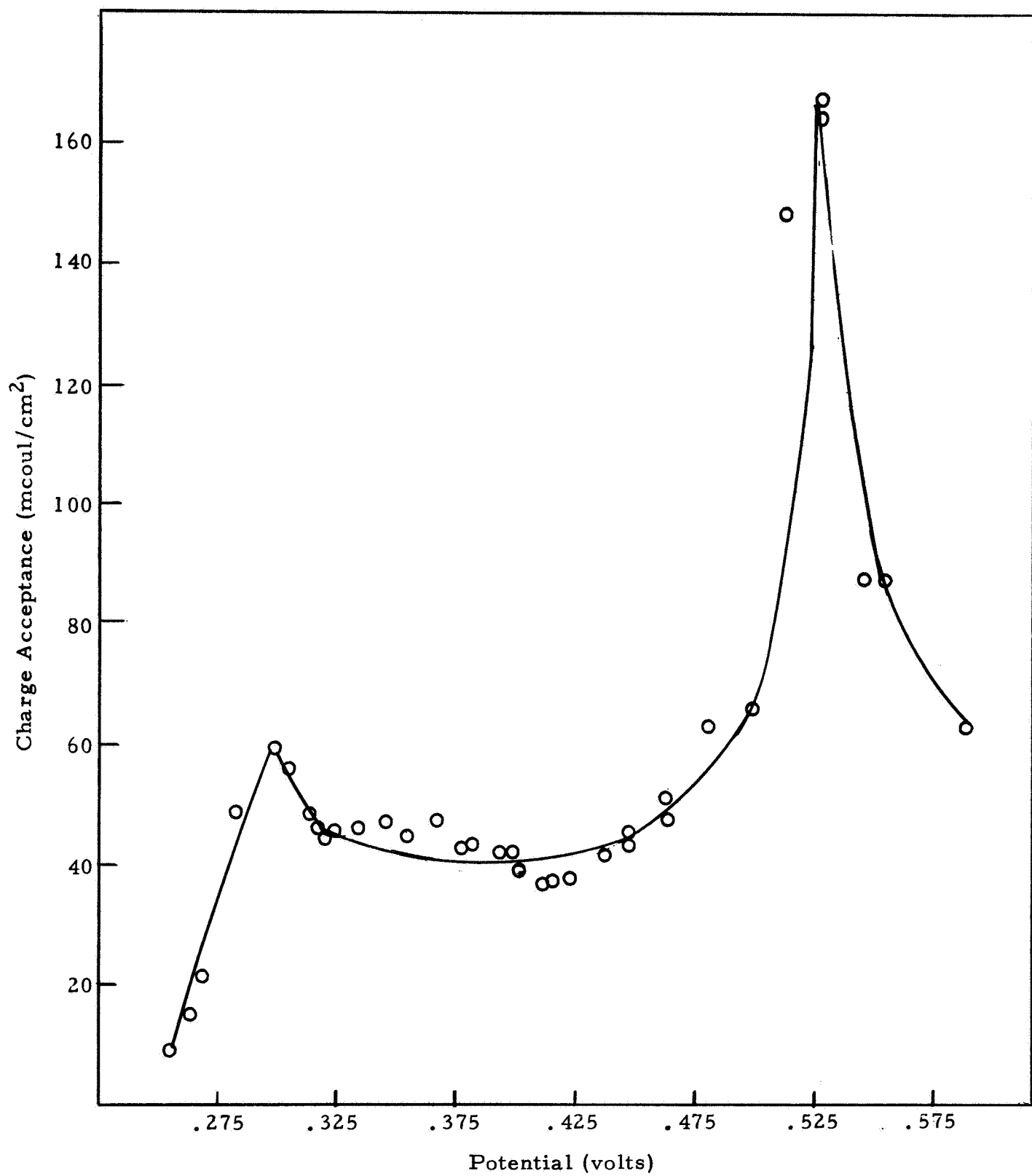


Fig. 9. --Charge acceptance per unit area of silver-on-glass electrodes as a function of applied potential.

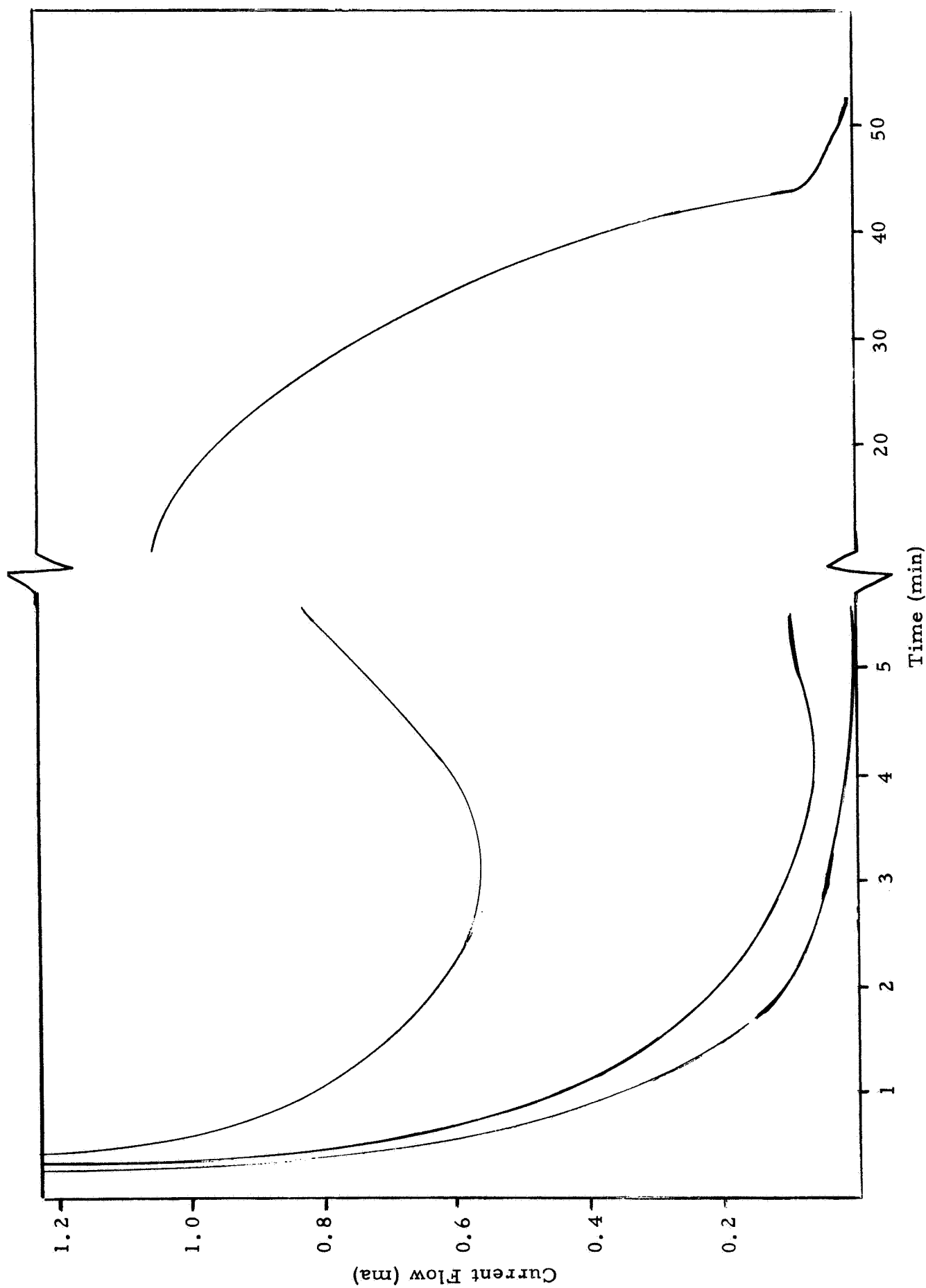


Fig.10. ---Current flow in the electrolytic oxidation of silver surfaces at a constant potential of 0.320 volt.
 A. Silver-on-glass electrode from vapor deposition C. Sintered silver electrodes --Delco Remy
 B. Silver foil etched in 6N HNO_3 for 120 sec.

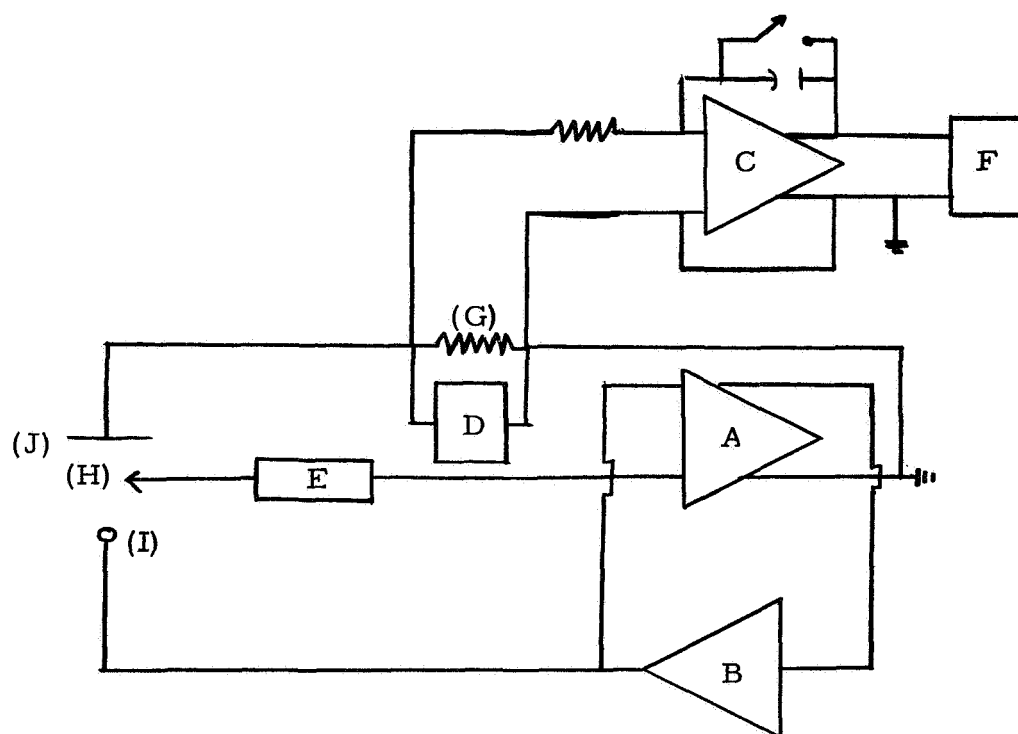


Fig.11 . --Circuit of Potentiostat with 100 ma Booster Amplifier

- (A) Potentiostat--Philbrick P25AU Operational Amplifier
- (B) Booster--Philbrick P66A Power Amplifier (100 ma mode)
- (C) Integrator--Philbrick P25AU Operational Amplifier
- (D) Current Recorder
- (E) Constant Potential Power Supply
- (F) Integrator Output Recorder
- (G) 100 Ohm Standard Resistor
- (H) Hg-HgO Reference Electrode
- (I) Silver Working Electrode
- (J) Platinum Counter Electrode

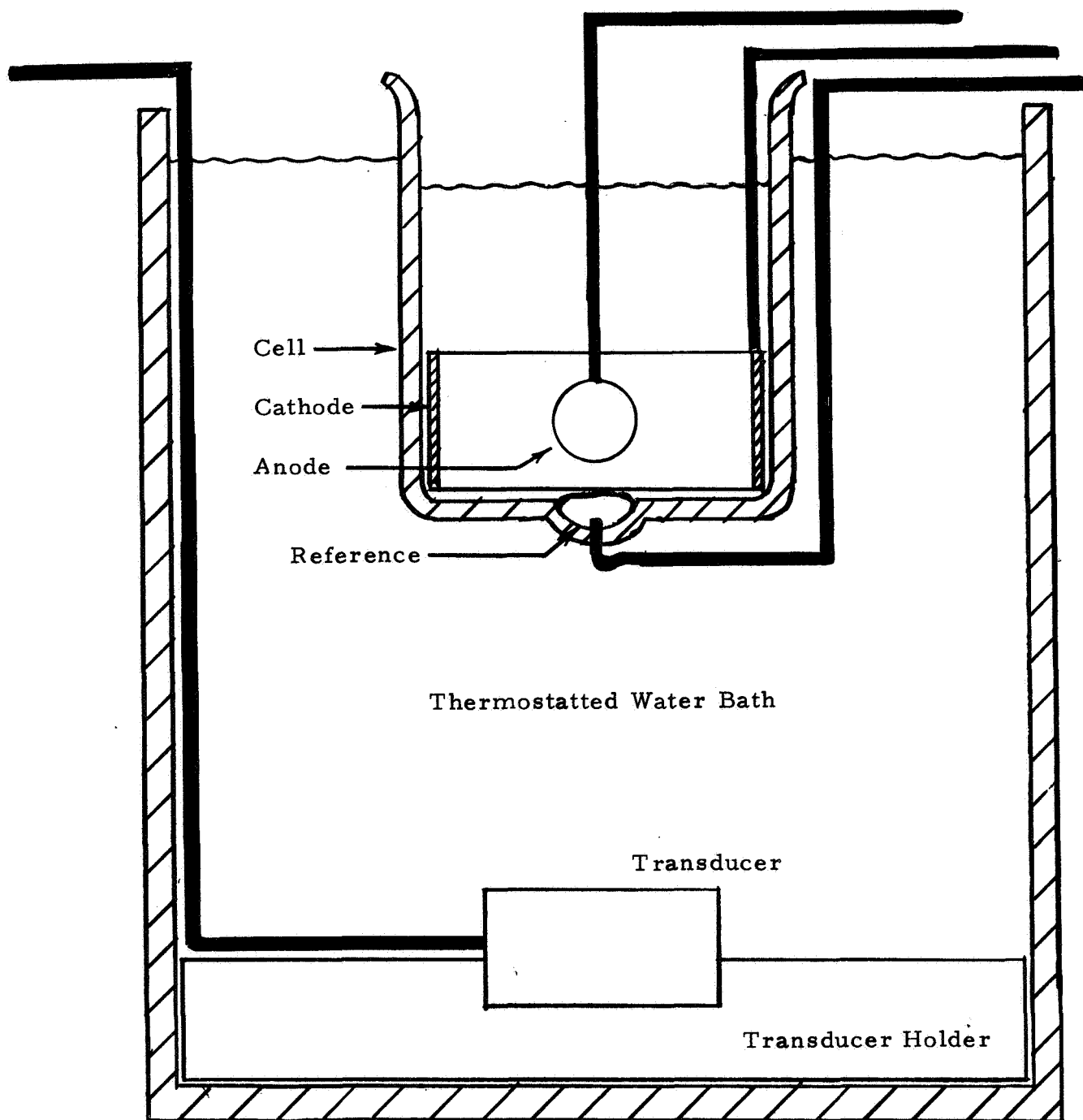
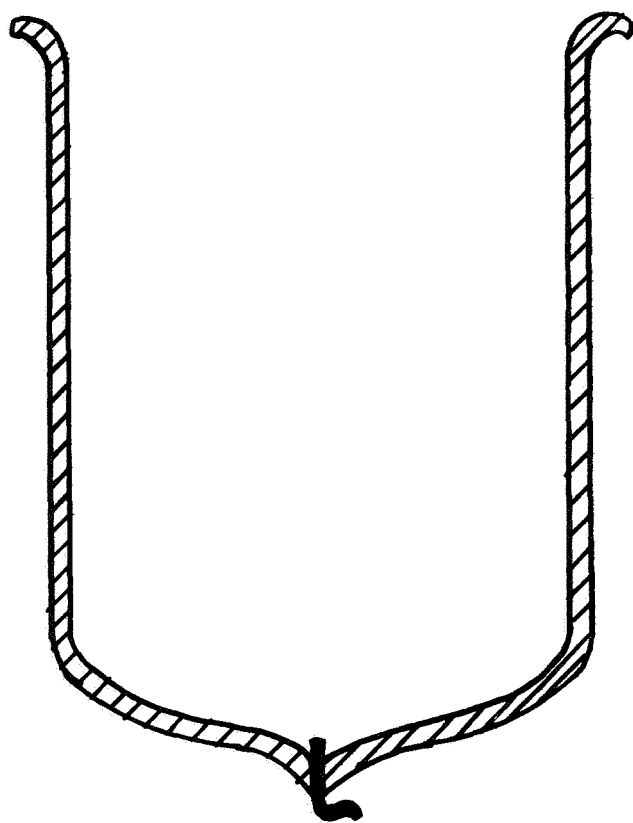
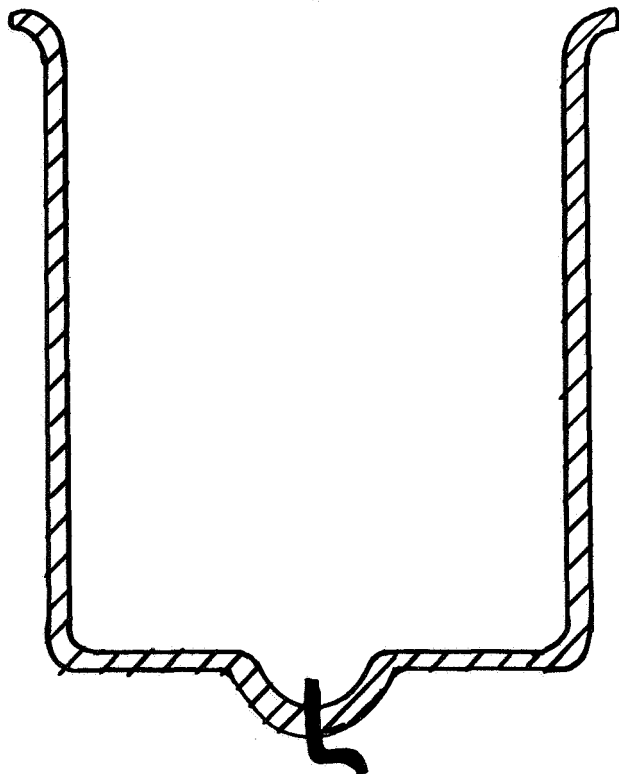


Fig. 12. --Thermostatted bath showing transducer, cell, and electrodes .



A

Round Bottomed Cell



B

Flat Bottomed Cell

Fig. 13. --Two types of cell design .

REFERENCES

1. M. D. Wijnen and W. M. Smit, Recueil, 79, 22 (1960).
2. E. A. Butler and A. U. Blackham, "Studies of Reaction Geometry in Oxidation and Reduction of the Alkaline Silver Electrode", First Quarterly Report, JPL 952268, August 15, 1968.
3. Ibid., Final Report, JPL 951911, May 15, 1968.
4. W. Vielstich and H. Gerischer, Z. physik. Chem. Neue Folge, 4, 10 (1955).
5. P. A. Malachesky and R. Jasinski, Tyco Lab., Inc., Waltham, Mass; Abs. No. 174, Electrochemical Society Inc., Spring Meeting, Boston, Mass., May 5-9, 1968.
6. (a) C. P. Wales and A. C. Simon, "Crystallographic Changes During Oxidation (Charging) of the Silver Electrode", Part 2--Oxidation Following Five Charge-Discharge Cycles at a Low Rate, NRL 6707, May 13, 1968.
(b) C. P. Wales, Private Communication, October 14, 1968.
7. E. A. Butler and A. U. Blackham, "Studies of Reaction Geometry in Oxidation and Reduction of the Alkaline Silver Electrode", Final Report, JPL 951554, April 10, 1967.
8. M. F. Skalozubov, F. I. Kukoz, and G. V. Mikhailenko, Akad. Nauk SSSR, Otd. Obshch. i Tekhn. Khim. Sb. Statei, 1965, 280, C. A. 65:4997e (1966).
9. R. C. Alkire, E. A. Grens, and C. W. Tobias, Abstract No. 366, The Electrochemical Society, Inc., Fall Meeting, Montreal, Oct. 6-11, 1968, p. 227, 228.
10. P. Delahay, "New Instrumental Methods in Electrochemistry", Interscience Publishers, Inc., New York, 1965, p. 36.